Thermal electron acceleration by localized bursts of electric field in the radiation belts

A.V. Artemyev, O. V. Agapitov, F Mozer, V Krasnoselskikh

▶ **To cite this version:**

A.V. Artemyev, O. V. Agapitov, F Mozer, V Krasnoselskikh. Thermal electron acceleration by localized bursts of electric field in the radiation belts. Geophysical Research Letters, 2014, 41, pp.5734-5739. 10.1002/2014GL061248 . insu-01171225

HAL Id: insu-01171225

https://insu.hal.science/insu-01171225

Submitted on 3 Jul 2015

HAL is a multi-disciplinary open access archive for the deposit and dissemination of scientific research documents, whether they are published or not. The documents may come from teaching and research institutions in France or abroad, or from public or private research centers.

L'archive ouverte pluridisciplinaire **HAL**, est destinée au dépôt et à la diffusion de documents scientifiques de niveau recherche, publiés ou non, émanant des établissements d'enseignement et de recherche français ou étrangers, des laboratoires publics ou privés.

AGU PUBLICATIONS

Geophysical Research Letters

RESEARCH LETTER
10.1002/2014GL061248

Key Points:
- Observation of high-amplitude electrostatic structures in radiation belts
- Thermal electron resonance acceleration by electrostatic structures
- Formation of seed population for further acceleration by whistler waves

Correspondence to:
A. V. Artemyev,
ante0226@gmail.com

Citation:
Artemyev, A. V., O. V. Agapitov, F. Mozer, and V. Krasnoselskikh (2014), Thermal electron acceleration by localized bursts of electric field in the radiation belts, *Geophys. Res. Lett.*, *41*, 5734–5739, doi:10.1002/2014GL061248.

Received 17 JUL 2014
Accepted 9 AUG 2014
Accepted article online 13 AUG 2014
Published online 27 AUG 2014

Thermal electron acceleration by localized bursts of electric field in the radiation belts

A. V. Artemyev[1], O. V. Agapitov[2,3], F. Mozer[2], and V. Krasnoselskikh[4]

[1]Space Research Institute, RAS, Moscow, Russia, [2]Space Sciences Laboratory, University of California, Berkeley, California, USA, [3]Astronomy and Space Physics Department, Taras Shevchenko National University of Kiev, Kiev, Ukraine, [4]LPC2E/CNRS, University of Orleans, Orleans, France

Abstract In this paper we investigate the resonant interaction of thermal ~10–100 eV electrons with a burst of electrostatic field that results in electron acceleration to kilovolt energies. This single burst contains a large parallel electric field of one sign and a much smaller, longer-lasting parallel field of the opposite sign. The Van Allen Probe spacecraft often observes clusters of spatially localized bursts in the Earth's outer radiation belts. These structures propagate mostly away from the geomagnetic equator and share properties of soliton-like nonlinear electron acoustic waves: a velocity of propagation is about the thermal velocity of cold electrons (~3000–10,000 km/s), and a spatial scale of electric field localization along the field lines is about the Debye radius of hot electrons (~5–30 km). We model the nonlinear resonant interaction of these electric field structures and cold background electrons.

1. Introduction

Electric time domain structures consist of packets of electric field spikes, each spike having a duration of the order of hundreds of microseconds and, most importantly, containing a local parallel (to the magnetic field) electric field. In this paper we consider electrostatic time domain structures characterized mainly by bursts of parallel electrostatic field (BEF) components. These bursts are capable of accelerating electrons to keV energies through resonance of the moving electrons with a BEF traveling along the magnetic field at the same velocity, even if the BEF contains no net potential. This result will be shown by considering a model of BEF moving away from the equator with a velocity comparable to that of thermal (10–100 eV) electrons.

In the vicinity of the resonance, where the electron parallel velocity is equal to the velocity of BEF propagation, the electron dynamics are determined by the competition of the electrostatic field and mirror force due to the background magnetic field inhomogeneity. For strong enough BEF, the electrostatic field compensates the action of the mirror force and an electron becomes trapped into the resonance. Such an electron moves away from the equator into a region of stronger magnetic field, and its parallel velocity is converted to perpendicular velocity by conservation of the first adiabatic invariant. Thus, the process combines parallel acceleration and transformation of parallel energy to perpendicular energy while keeping the parallel velocity close to the BEF velocity for a period of trapping during which the particle is continuously accelerated by the BEF electric field, which can be as large as 100 mV/m. The rate of such acceleration is determined by the rate of the parallel velocity conversion to perpendicular velocity. Thus, the timescale of the acceleration is comparable with a fourth of an electron bounce period (about 1 s for cold electrons). The total energy of accelerated electrons can substantially exceed a potential drop across the single BEF and is determined by the relation between the electrostatic field and the inhomogeneity of the background magnetic field.

It will be shown that this process occurs in the Earth's outer radiation belt to be an important source of seed particles that are accelerated to relativistic energies in a similar resonance process with whistler mode waves. It is emphasized that BEFs are observed in the outer radiation belts [*Mozer et al.*, 2013, 2014; *Malaspina et al.*, 2014], the auroral zone [*Ergun et al.*, 1998], the reconnecting magnetopause [*Mozer and Pritchett*, 2009], and magnetotail [*Matsumoto et al.*, 1994; *Khotyaintsev et al.*, 2010], in the bow shock [*Bale et al.*, 1998] and in many current-carrying environments, so this process of resonant interaction between electrons and BEF may be important in many different physical regimes.

2. Observations

Van Allen probes A and B were launched on 30 August 2012. During the intervals discussed below, the ambient magnetic field was within 10° of the satellite spin plane (the plane approximately normal to the

©2014. American Geophysical Union. All Rights Reserved.

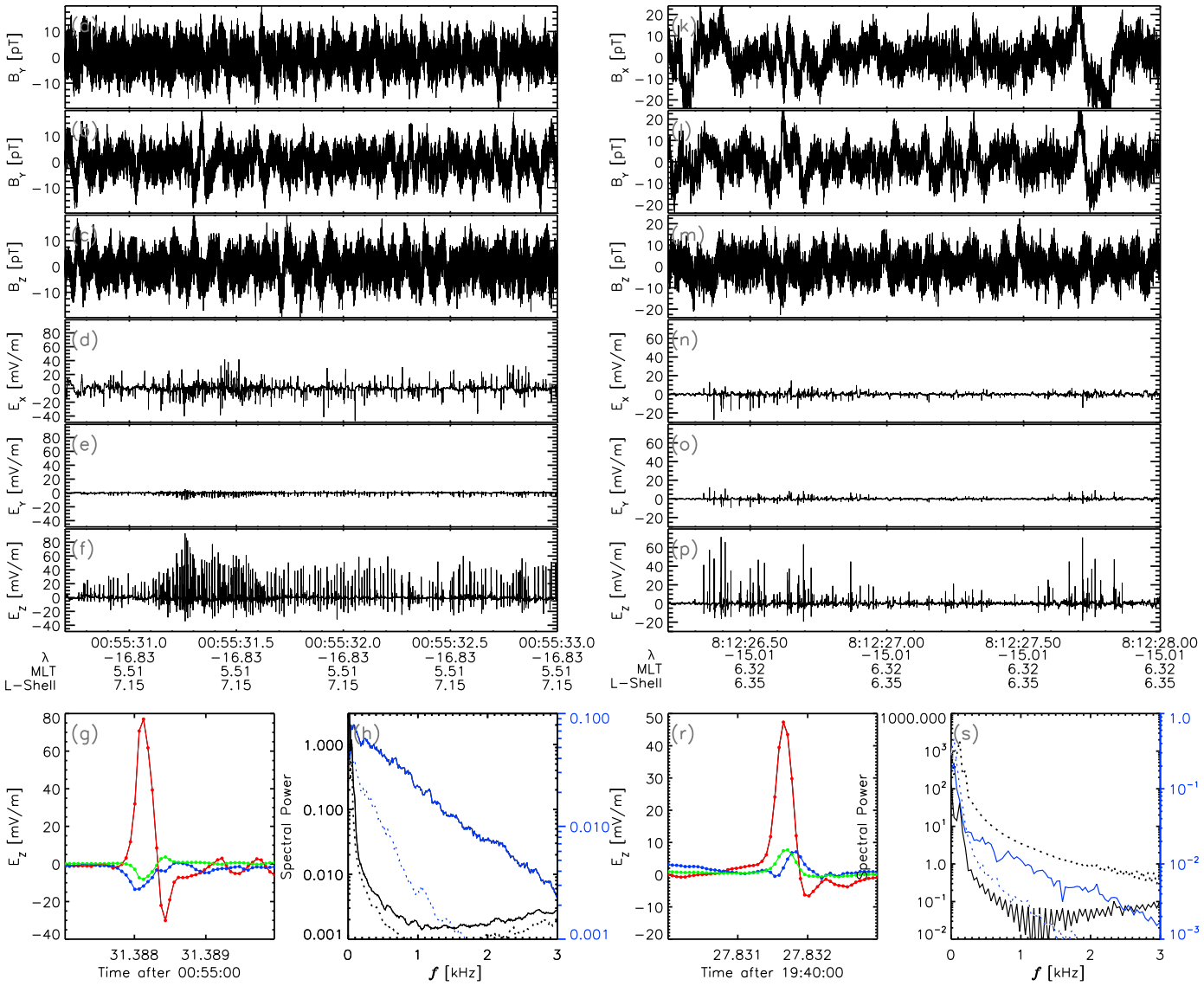

Figure 1. BEFs observed aboard VAPB (a–h) on 13 November 2012 and (k–s) on 1 November 2012. Figures 1a–1c show three components of the magnetic field while the electric field in the background magnetic field-aligned coordinates is illustrated in Figures 1d–1f (E_z is the parallel component, and E_x, E_y are transverse components). Figure 1g shows 3 ms of electric field observations. Parallel component is indicated by red color; transverse component are indicated by blue and green. The spectra of magnetic and electric field perturbations are shown in Figure 1h by black and blue curves respectively with corresponding black and blues scales in pT^2/Hz and mV^2/m^2Hz. Solid curves indicate parallel perturbations, and dashed curves indicate transverse ones.

Sun-Earth line) and the spin plane contained electric field measuring spheres 1, 2, 3, and 4, each at the end of a 50 m wire while shorter booms with spheres on their ends were located parallel to the spin axis [*Wygant et al.*, 2013]. The electric field data were transmitted at 16,384 samples/s for 5 s intervals in a burst mode. Search coil magnetic field data [*Kletzing et al.*, 2013] were also transmitted through the electric field instrument at the same time and data rate as the electric field measurement. The search coil data were corrected for the frequency response of this measurement and verified by comparison to higher-frequency bursts from the magnetic field instrument.

Figure 1 illustrates the three fluctuating components of the electric and magnetic fields in the background magnetic field-aligned coordinates during a 1 s interval on 13 November and 1 November 2012 (see also *Mozer et al.* [2013] for detailed information on the second case). Figures 1a and 1b (1k and 1l) give the perpendicular components of the magnetic field (*X* and *Y* components in Figure 1) and the parallel *Z* component is given in Figure 1c (1m). Figures 1d and 1e (1n and 1o) give the two perpendicular components of the electric field and Figure 1f (1p) gives the parallel (to the background magnetic field) component.

©2014. American Geophysical Union. All Rights Reserved.

In Figure 1g (1r), a 3 ms zoom of the electric field observations is shown. The frequency range of BEF corresponds to 300–1000 Hz. In this frequency range the relation of magnetic and electric field amplitudes presented in Figures 1h and 1s ($|\mathbf{B}| \sim 0.1$ pT^2/Hz and $|\mathbf{E}| \sim 0.1 - 1$ mV^2/m^{2}Hz) suggests that these are electrostatic structures. The main electric field perturbation component, E_z, is along the background magnetic field (see Figures 1f and 1p). For some BEF, we observe peaks of the transverse electric field component with an amplitude up to 30% of the maximum value of E_z. However, there are a lot of BEFs with almost parallel electric field. Two examples of such BEFs are shown in Figures 1g and 1r. (The undershoots following the positive BEF signals arise from the fact that the data are ac coupled so there is no net signal.) The duration of a single BEF (∼1 ms) and an estimate of the propagation velocity (from the time shift of signals on different antennas (as described in *Mozer et al.* [2013])) $v_\phi \sim$ 2000–10,000 km/s gives a spatial scale of about l∼5–10 km along the background magnetic field. However, we should mention that the error can be large for $v_\phi > 5000$ km/s (when the time shift is less than the measurements sampling time), but for v_ϕ less than 5000 km/s the timing gives robust results. The direction of BEF propagation is evaluated using waveform timing. The propagation velocity and spatial scales are well described in terms of nonlinear electron acoustic waves supported by ∼100 eV cold electrons and populations of ∼1–10 keV hot electrons [*Fried and Gould*, 1961; *Lashmore-Davies and Martin*, 1973]. The two cases presented in Figure 1 therefore show the nonlinear structures propagating from the geomagnetic equator with velocity ∼2000 km/s for the first case and ∼4000 km/s for the second.

3. Model of the Landau Resonance

Our model deals with the nonlinear interaction of electrons with moving BEF. BEF are observed up to 20° of latitudes (see Figure 1) and in the auroral latitudes (up to 70°) by Polar [*Mozer et al.*, 1997] as well as by FAST [*Ergun et al.*, 1998]. There is no clear dependence of their amplitude on latitude. Thus, we assume that BEF are propagating to high latitudes with constant amplitudes. To describe such an interaction we introduce the simplified model of the scalar potential for the single BEF $\Phi = \Phi_0 F(\phi)$, where $\phi = (z - u_\phi t)/l$, z is the coordinate along the field line, and u_ϕ is the velocity of BEF motion. Dependence of ϕ only on the parallel coordinate z corresponds to the absence of transverse electric field components associated with BEF. We assume that l and u_ϕ do not vary along field lines (this assumption is based on the dispersion properties of electron acoustic waves [*Fried and Gould*, 1961; *Lashmore-Davies and Martin*, 1973]). The spatial localization of BEF across the magnetic field lines is supposed to be substantially larger than the parallel scale l (see nonliner models of BEF and BEF-like structures in *Jovanović and Shukla* [2000] and *Jovanović and Krasnoselskikh* [2009]). Thus, we can consider electron resonant interaction with a single BEF within the approximation of the system homogeneity across the field lines.

The function $f = \mathrm{d}F/\mathrm{d}\phi$ determines the profile of the electric field. We choose $F(\phi)$ in such a way that $F \to 0$ for $\phi \to \pm\infty$ (there is no net potential across the structure) and $\mathrm{d}F/\mathrm{d}\phi$ has the strong positive peak and wide negative tail: $F(\phi) = \exp(-\phi^2)(\tanh(\sigma\phi) - 1)$, where $\sigma \gg 1$. Model profiles of Φ and the electric field $E_\parallel = -(\Phi_0\sigma/l)f(\phi)$ are shown in Figure 2a. We consider nonrelativistic electron motion in the dipole magnetic field with the magnitude $B(z) = B_{\mathrm{eq}}b(z)$. We concentrate on Landau resonant interaction of BEF with electrons; thus, electron gyrorotation is not perturbed and the magnetic moment $\mu = m_e v_0^2 \sin^2\alpha_{\mathrm{eq}}/2B_{\mathrm{eq}}$ is conserved (here m_e is the electron mass, $v_0 = \sqrt{2H_0/m_e}$ is the amplitude of the electron velocity, H_0 is the initial energy, and α_{eq} is the electron equatorial pitch angle). The Hamiltonian of the electron motion can be written as

$$H = \frac{1}{2}m_e\left(\frac{\mathrm{d}z}{\mathrm{d}t}\right)^2 + \mu B(z) - e\Phi_0 F(\phi) \tag{1}$$

We introduce the dimensionless variables and parameters $z/R = s$, $u_\phi/v_0 = v_\phi$, $tv_0/R = \tau$, $\varepsilon = 2e\Phi_0\sigma R/lv_0^2 m_e$ (here $R = R_E L$ is the spatial scale of the dipole magnetic field variation) and we write the equation of electron motion as

$$\frac{\mathrm{d}^2 s}{\mathrm{d}\tau^2} = -\frac{1}{2}\sin^2\alpha_{\mathrm{eq}}\frac{\mathrm{d}}{\mathrm{d}s} + \frac{1}{2}\varepsilon f(\phi) \tag{2}$$

with $\phi = (s - v_\phi\tau)R/l$ and $R/l \gg 1$. A large value of R/l provides the fast change of the phase ($\mathrm{d}\phi/\mathrm{d}\tau \sim R/L \gg \mathrm{d}s/\mathrm{d}\tau$). Thus, we can assume that ϕ is the fast phase and s is a slow variable. In this case, in the

©2014. American Geophysical Union. All Rights Reserved.

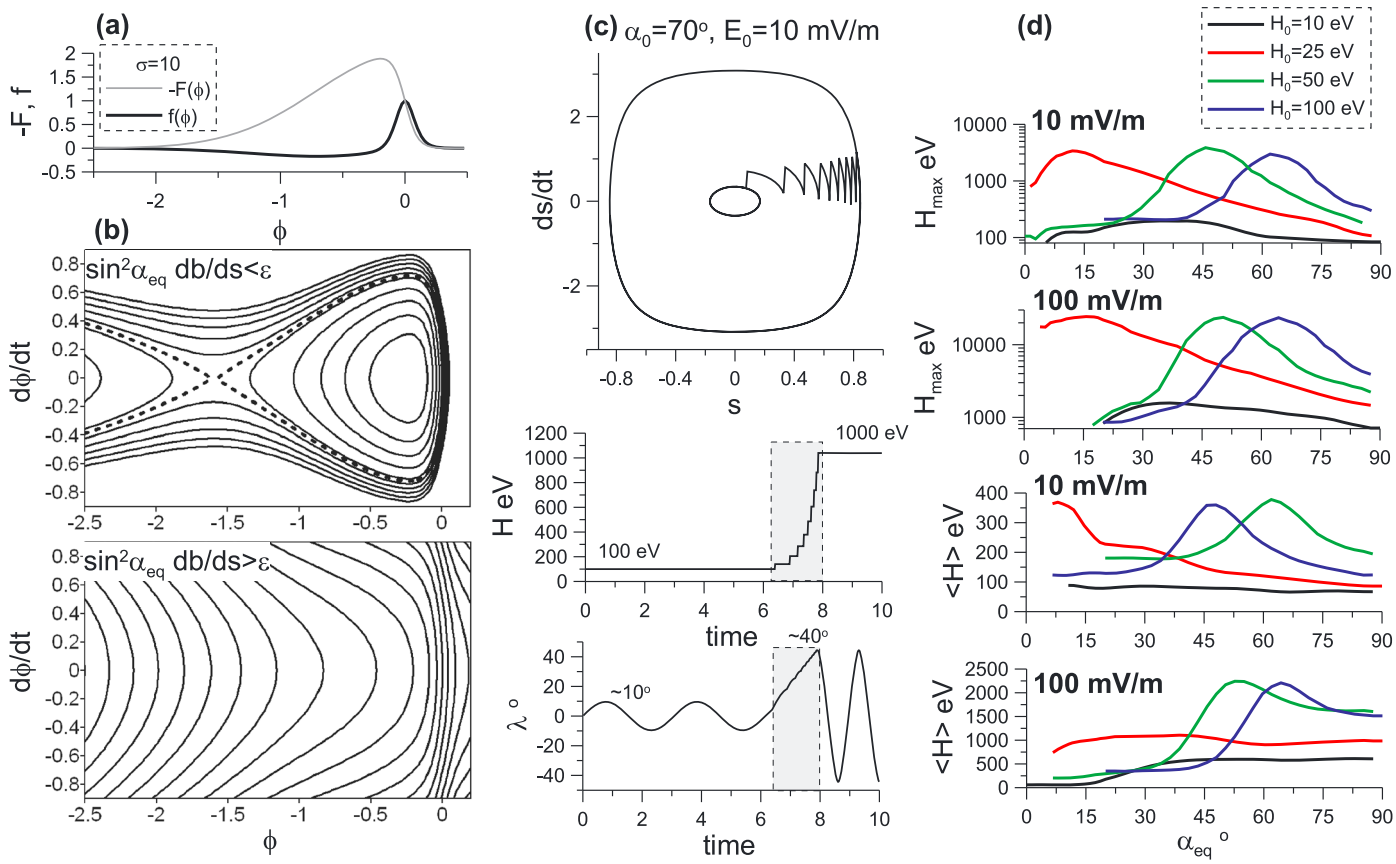

Figure 2. (a) Profiles of the model electric field $f(\phi)$ and the scalar potential $F(\phi)$. (b) Phase portraits of system described by equation (4). (c) An example of particle trajectories in the plane $(s, \mathrm{d}s/\mathrm{d}\tau)$, the particle energy as functions of time, particle latitudes λ as functions of time. Trajectories are obtained by numerical integration of equation (2) with $l = 5$ km, $R_0 = 5R_E$. The grey color shows the time interval of particle trapping. (d) Maximum and averaged energies gained by particles having initial energies of 10 ev, 25 ev, 50 ev, and 100 ev as a function of initial equatorial pitch angle. Two values of electric field amplitude are considered. Each point is obtained by numerical integration of 10^3 trajectories.

vicinity of the resonance $\mathrm{d}\phi/\mathrm{d}\tau = 0$ and equation(2) takes a form

$$\frac{\mathrm{d}^2\phi}{\mathrm{d}\tau^2} = -\frac{R}{2l}\left(\sin^2\alpha_{\mathrm{eq}}\frac{\mathrm{d}b}{\mathrm{d}s} - \varepsilon f(\phi)\right) \tag{3}$$

And the corresponding Hamiltonian is

$$H_\phi = \frac{1}{2}\left(\frac{\mathrm{d}\phi}{\mathrm{d}\tau}\right)^2 + \frac{R}{2l}\left(\sin^2\alpha_{\mathrm{eq}}\frac{\mathrm{d}b}{\mathrm{d}s}\phi - \varepsilon F(\phi)\right) \tag{4}$$

The phase portrait of the Hamiltonian (4) is shown in Figure 2b for two cases: $\sin^2\alpha_{\mathrm{eq}}(\mathrm{d}b/\mathrm{d}s) > \varepsilon$ and $\sin^2\alpha_{\mathrm{eq}}(\mathrm{d}b/\mathrm{d}s) < \varepsilon$. In the second case, there is a region of closed trajectories corresponding to trapped particles. Thus, particles can be trapped by the electrostatic structure and accelerated along field lines (this is essentially the same mechanism as that considered for relativistic electron acceleration by oblique whistler waves [see *Shklyar and Matsumoto*, 2009; *Artemyev et al.*, 2012, and references therein]). An example of particle trapping and acceleration is shown in Figure 2c in which a particle oscillate between mirror points (closed trajectories in the $(s, \mathrm{d}s/\mathrm{d}\tau)$ plane), before becoming trapped to move with the electrostatic structure to high latitudes. The particle escapes from the resonance at high latitude (see the third panel of Figure 2c) when $\mathrm{d}b/\mathrm{d}s$ becomes large enough to remove closed trajectories from the phase portrait, as in Figure 2b. During this one trapping-escape event the particle gains around ~1 keV; see the second panel of Figure 2c.

The dependence of the acceleration rate on system parameters is given by the expression $\Delta H = H_0(b(s_{\mathrm{esc}}) - b(s_{\mathrm{trap}}))\sin^2\alpha_{\mathrm{eq}}$ where s_{trap} and s_{esc} are coordinates of trapping into the resonance and escape from the

©2014. American Geophysical Union. All Rights Reserved.

resonance (see more general equation with $I = I(s)$ in *Shklyar and Matsumoto* [2009]). To determine the position of trapping s_{trap} one needs to consider the moment of the formation of the electrostatic structure (i.e., growth of the amplitude ε from small value $\varepsilon < \sin^2 \alpha_{eq}(db/ds)_{s_{trap}}$ to larger value $\varepsilon > \sin^2 \alpha_{eq}(db/ds)_{s_{trap}}$; see detailed description of this process for electrostatic whistler waves in *Artemyev et al.* [2013] and *Agapitov et al.* [2014]). To determine the position of escape from the resonance one should consider the particle oscillation in the phase plane $(\phi, d\phi/dt)$ with slowly changing $b(s)$ [see *Artemyev et al.*, 2013]. Both of these positions s_{trap}, s_{esc} can be found analytically only with the help of a more comprehensive model of the electrostatic structure. In this paper we use our simplified model to obtain the maximum possible energy in numerical calculations. We consider four values of initial energies (10 eV, 25 eV, 50 eV, and 100 eV) and 45 values of equatorial pitch angles. For each value of pitch angle and energy, we ran 10^3 trajectories with the different initial phases ϕ. All trajectories were integrated during one bounce period, and energies of the most accelerated particles were recorded. We also calculated the average energy of the accelerated particles. The final results, shown in Figure 2d, demonstrate that particles can gain up to 1–10 keV for typical amplitudes of the electric field. The first and second panels in Figure 2d show the dependence of the maximum possible gain of energy as a function of the initial equatorial pitch angle α_{eq} for two values of a BEF amplitude. The four curves correspond to four values of the initial particle energy (10 eV, 25 eV, 50 eV, and 100 eV). The maximum of energy depends on α_{eq} nonmonotonically: for each initial energy, there is a maximum of gained energy for a particular value of equatorial pitch angle. For small pitch angles, the final energy is small due to the dependence $\Delta H \sim \sin^2 \alpha_{eq}$, while large pitch angles correspond to lower latitudes (smaller s_{esc}) of particle escape from the resonance and, as a result, to smaller $\Delta H \sim b(s_{esc})$. For each initial energy, the pitch angle corresponding to the maximum energy gain is different. The third and fourth panels in Figure 2d show profiles of the average energy of accelerated particles as functions of α_{eq} for two values of a BEF amplitude. The average gained energy varies from 100 eV (for the wave amplitude ~10 mV/m) up to 1000–2000 eV (for the wave amplitude ~100 mV/m). These values are several times smaller than values of the maximum gained energy.

4. Discussion and Conclusions

In this paper we have shown that small-scale bursts of parallel electric field (presumably related to nonlinear electron acoustic waves) can effectively accelerate electrons via the Landau resonance even if there is no net potential in the structure. This acceleration mechanism can have direct application to the Earth's radiation belts where formation of the keV electron population is an important question [e.g., *Mozer et al.*, 2014]. We also mention additional possible applications of the proposed model. Electric field structures of the type described in this paper are observed in the vicinity of the reconnection region [*Mozer and Pritchett*, 2009; *Khotyaintsev et al.*, 2010] and during magnetic field dipolarization [*Deng et al.*, 2010] in the Earth's magnetotail. Thus, the dominance of electron acceleration parallel to the magnetic field during reconnection and dipolarization [*Asano et al.*, 2010; *Runov et al.*, 2013] might also be due to nonlinear trapping of electrons into the Landau resonance. In contrast to electron resonant scattering by whistler waves, the electron nonlinear interaction with electrostatic structures cannot be described in quasi-linear theory because the single act of interaction results in an electron energy change comparable to the initial energy. Thus, one should suggest an alternative approach to incorporate this nonlinear interaction into the Fokker-Planck equation for electrons. One possible way is to determine the probabilities of particle trapping by these electric field structures and introduce the additional operator into the Fokker-Planck equation to model rapid particle transport in phase space (see details of such an approach in *Shklyar* [1981] and *Artemyev et al.* [2013]). It is also unclear whether and how to include the nonlinear effects of damping and amplification of these electric structures due to currents of trapped and transient particles [*Omura et al.*, 2008; *Shklyar*, 2011]. Such effects can be very important because, in comparison to the whistler wave acceleration operating with high-energy electrons, our model explains the efficient acceleration of thermal electrons. That means the acceleration process can strongly modify the major part of the electron distribution and change macroscopic parameters such as the electron temperature and the heat flux.

In this paper we have estimated the energy gain due to the interaction of electrons with a single BEF. However, as Figure 1 shows, the BEFs occur in packets whose numbers can be hundreds or thousands of BEFs. Thus, an electron that does not achieve the maximum energy in a single interaction may go on to interact with other BEFs such that a large fraction of the incidence electrons may be accelerated to nearly the maximum energy.

©2014. American Geophysical Union. All Rights Reserved.

To conclude, we have presented the observations of large amplitude electric field structures in the radiation belts. We have shown that these structures share some properties typical of nonlinear soliton-like electron acoustic waves. Based on the observed properties of these electric field structures we consider the possible electron resonant acceleration via the Landau resonance. Initially cold (thermal) electrons with an energy ~10–100 eV can gain up to few keVs during a single nonlinear trapping event. This mechanism of acceleration potentially can be responsible for the formation of superthermal electron populations with energies ~1 keV.

Acknowledgments
The work by O.A. and F.M. was performed under JHU/APL contract 922613 (RBSP-EFW). The work of A.V.A was partially supported by MK-1781.2014.2. The authors thank all the people associated with the electric field, magnetic field, and particle teams on the Van Allen probes and to the project team at the Johns Hopkins Applied Physics Laboratory that manages this program. All data used in this paper can be found at RBSP/EFW database (http://www.space.umn.edu/missions/rbspefw-home-university-of-minnesota/)

The Editor thanks two anonymous reviewers for their assistance in evaluating this paper.

References

Agapitov, O., A. Artemyev, D. Mourenas, V. Krasnoselskikh, J. Bonnell, O. Le Contel, C. M. Cully, and V. Angelopoulos (2014), The quasi-electrostatic mode of chorus waves and electron nonlinear acceleration, *J. Geophys. Res. Space Physics*, *119*, 1606–1626, doi:10.1002/2013JA019223.

Artemyev, A., V. Krasnoselskikh, O. Agapitov, D. Mourenas, and G. Rolland (2012), Non-diffusive resonant acceleration of electrons in the radiation belts, *Phys. Plasmas*, *19*, 122901, doi:10.1063/1.4769726.

Artemyev, A. V., A. A. Vasiliev, D. Mourenas, O. Agapitov, and V. Krasnoselskikh (2013), Nonlinear electron acceleration by oblique whistler waves: Landau resonance vs. cyclotron resonance, *Phys. Plasmas*, *20*, 122901, doi:10.1063/1.4836595.

Asano, Y., et al. (2010), Electron acceleration signatures in the magnetotail associated with substorms, *J. Geophys. Res.*, *115*, A05215, doi:10.1029/2009JA014587.

Bale, S. D., P. J. Kellogg, D. E. Larsen, R. P. Lin, K. Goetz, and R. P. Lepping (1998), Bipolar electrostatic structures in the shock transition region: Evidence of electron phase space holes, *Geophys. Res. Lett.*, *25*, 2929–2932, doi:10.1029/98GL02111.

Deng, X., M. Ashour-Abdalla, M. Zhou, R. Walker, M. El-Alaoui, V. Angelopoulos, R. E. Ergun, and D. Schriver (2010), Wave and particle characteristics of earthward electron injections associated with dipolarization fronts, *J. Geophys. Res.*, *115*, A09225, doi:10.1029/2009JA015107.

Ergun, R. E., et al. (1998), FAST satellite observations of large-amplitude solitary structures, *Geophys. Res. Lett.*, *25*, 2041–2044, doi:10.1029/98GL00636.

Jovanović, D., and P. K. Shukla (2000), Nonlinear model for coherent electric field structures in the magnetosphere, *Phys. Rev. Lett.*, *84*, 4373–4376, doi:10.1103/PhysRevLett.84.4373.

Jovanović, D., and V. V. Krasnoselskikh (2009), Kinetic theory for the ion humps at the foot of the Earth's bow shock, *Phys. Plasmas*, *16*, 102902, doi:10.1063/1.3240342.

Fried, B. D., and R. W. Gould (1961), Longitudinal ion oscillations in a hot plasma, *Phys. Fluids*, *4*, 139–147, doi:10.1063/1.1706174.

Khotyaintsev, Y. V., A. Vaivads, M. André, M. Fujimoto, A. Retinò, and C. J. Owen (2010), Observations of slow electron holes at a magnetic reconnection site, *Phys. Rev. Lett.*, *105*(16), 165002, doi:10.1103/PhysRevLett.105.165002.

Kletzing, C. A., et al. (2013), The electric and magnetic field instrument suite and integrated science (EMFISIS) on RBSP, *Space Sci. Rev.*, *179*, 127–181, doi:10.1007/s11214-013-9993-6.

Lashmore-Davies, C., and T. Martin (1973), Electrostatic instabilities driven by an electric current perpendicular to a magnetic field, *Nucl. Fusion*, *13*(2), 193.

Malaspina, D. M., et al. (2014), Nonlinear electric field structures in the inner magnetosphere, *Geophys. Res. Lett.*, *41*, doi:10.1002/2014GL061109.

Matsumoto, H., H. Kojima, T. Miyatake, Y. Omura, M. Okada, I. Nagano, and M. Tsutsui (1994), Electrotastic solitary waves (ESW) in the magnetotail: BEN wave forms observed by GEOTAIL, *Geophys. Res. Lett.*, *21*, 2915–2918, doi:10.1029/94GL01284.

Mozer, F. S., R. Ergun, M. Temerin, C. Cattell, J. Dombeck, and J. Wygant (1997), New features of time domain electric-field structures in the auroral acceleration region, *Phys. Rev. Lett.*, *79*, 1281–1284, doi:10.1103/PhysRevLett.79.1281.

Mozer, F. S., and P. L. Pritchett (2009), Regions associated with electron physics in asymmetric magnetic field reconnection, *Geophys. Res. Lett.*, *36*, L07102, doi:10.1029/2009GL037463.

Mozer, F. S., S. D. Bale, J. W. Bonnell, C. C. Chaston, I. Roth, and J. Wygant (2013), Megavolt parallel potentials arising from double-layer streams in the Earth's outer radiation belt, *Phys. Rev. Lett.*, *111*(23), 235002, doi:10.1103/PhysRevLett.111.235002.

Mozer, F. S., O. Agapitov, V. Krasnoselskikh, S. Lejosne, G. D. Reeves, and I. Roth (2014), Direct observation of radiation belt electron acceleration from electron volt energies to megavolts by non-linear whistlers, *Phys. Rev. Lett.*, *113*, 035001.

Omura, Y., Y. Katoh, and D. Summers (2008), Theory and simulation of the generation of whistler-mode chorus, *J. Geophys. Res.*, *113*, A04223, doi:10.1029/2007JA012622.

Runov, A., V. Angelopoulos, C. Gabrielse, X.-Z. Zhou, D. Turner, and F. Plaschke (2013), Electron fluxes and pitch-angle distributions at dipolarization fronts: THEMIS multipoint observations, *J. Geophys. Res. Space Physics*, *118*, 744–755, doi:10.1002/jgra.50121.

Shklyar, D., and H. Matsumoto (2009), Oblique whistler-mode waves in the inhomogeneous magnetospheric plasma: Resonant interactions with energetic charged particles, *Surv. Geophys.*, *30*, 55–104, doi:10.1007/s10712-009-9061-7.

Shklyar, D. R. (1981), Stochastic motion of relativistic particles in the field of a monochromatic wave, *Sov. Phys. JETP*, *53*, 1197–1192.

Shklyar, D. R. (2011), Wave-particle interactions in marginally unstable plasma as a means of energy transfer between energetic particle populations, *Phys. Lett. A*, *375*, 1583–1587, doi:10.1016/j.physleta.2011.02.067.

Wygant, J. R., et al. (2013), The electric field and waves instruments on the radiation belt storm probes mission, *Space Sci. Rev.*, *179*, 183–220, doi:10.1007/s11214-013-0013-7.

©2014. American Geophysical Union. All Rights Reserved.